DOI:
10.1002/mrm.26053

Document Version
Peer reviewed version

This is the author accepted manuscript version of Magn Reson Med 2016, DOI 10.1002/mrm.26053

Rapid Quantitative T_2 Mapping of the Prostate using 3D Dual Echo Steady State (DESS) MRI at 3T

Isabel Dregely*, Daniel AJ Margolis, Kyunghyun Sung, Ziwu Zhou,

Novena Rangwala, Steven S Raman, Holden H Wu

Department of Radiological Sciences, University of California Los Angeles, Los Angeles, California, USA

Running Head: Rapid DESS T_2 Mapping of the Prostate

Journal: Magnetic Resonance in Medicine

Word Count: Approximately 200 abstract, 3900 for body (not including title page, abstract, figure captions, tables, table captions, or references), 2 tables, 7 figures, 1 supporting table

Paper Type: Full Paper

*Correspondence to:

Isabel Dregely, PhD
Department of Radiological Sciences
300 UCLA Medical Plaza, Suite B109
Los Angeles, CA 90095
Phone: (310) 267-7009
Fax: (310) 825-9118
idregely@mednet.ucla.edu

This is the author accepted manuscript version of Magn Reson Med 2016, DOI 10.1002/mrm.26053

ABSTRACT

Purpose: To develop and evaluate a rapid 3D quantitative T_2 mapping method for prostate cancer imaging using Dual Echo Steady State (DESS) MRI at 3T.

Methods: In simulations, DESS-T_2 mapping in the presence of T_1 and B_1^+ variations was evaluated. In a phantom and healthy volunteers (n = 4), 3D DESS-T_2 mapping was compared to a 2D turbo spin echo (TSE) approach. In volunteers and a pilot patient study (n = 29), quantitative T_2 in normal prostate anatomical zones and in suspected cancerous lesions was evaluated.

Results: The simulated bias for DESS-T_2 was less than 2% (5%) for typically observed T_1 (B_1^+) variations. In phantoms and *in vivo*, high correlation of DESS-T_2 and TSE-T_2 (r^2 = 0.98 and 0.88, p-value < 0.001) was found. DESS-T_2 in the normal peripheral zone (PZ) / transition zone (TZ) was 115 ± 26 ms / 64 ± 7 ms in healthy volunteers and 129 ± 39 ms / 83 ± 12 ms in patients. In suspected cancerous lesions, DESS-T_2 was 72 ± 14 ms, which was significantly decreased from normal PZ ($p < 0.001$), but not from TZ.

Conclusion: Rapid 3D T_2 mapping in the entire prostate can be performed in one minute using DESS.

Keywords: Prostate Cancer Imaging, T_2 mapping, Dual Echo Steady State (DESS) MRI, and 3T MRI.

INTRODUCTION

Prostate cancer is the second leading cause of cancer related death in men in the U.S. (1). Conventionally, prostate cancer is diagnosed and monitored using transrectal ultrasonography (TRUS)-guided systematic needle biopsy to obtain tissue samples, which are assigned a Gleason Score (GS) indicating the aggressiveness of cancer. However, due to sampling bias this approach might miss clinically significant cancer and it is an uncomfortable, invasive procedure that some patients undergo repeatedly in conventional active surveillance. Magnetic Resonance Imaging (MRI) is a promising, non-invasive tool to detect and monitor prostate cancer (2). Prostate MRI relies on multi-parametric (mp) T_2-weighted (w), diffusion and dynamic contrast-enhanced imaging. However, qualitative analysis of mp-MRI alone performs suboptimally in distinguishing indolent from aggressive cancers. Le et al found that ~30% of clinically significant tumors (GS > 7 on whole-mount histopathology) were missed by multi-parametric MRI (mp-MRI) (3). Therefore, systematic biopsy is still considered the gold standard for assessing prostate cancer aggressiveness (4).

Quantitative MRI has shown promise for assessing tumor aggressiveness (5–9). Further, quantitative as opposed to qualitative MRI can reduce subjectivity in the assessment, which is important for long-term monitoring of patients such as men on active surveillance, as well as to improve uniformity of reporting across readers and institutions. However, the implementation of quantitative methods is technically challenging and thus far limited to research settings. One quantitative MR parameter, T_2 relaxation, reflects the interaction of water molecules on a cellular level and is therefore potentially highly sensitive to detect pathological tissue alterations. However, current methods to reliably measure T_2, such as single spin-echo (SE), acquire multiple image sets to map T_2. This results in compromises between spatial resolution, 3D coverage, and scan time. The impractically long scan times associated with SE-T_2 mapping, which might be on the order of tens of minutes, also make scans highly vulnerable to motion artifacts. Further, extracting T_2 from multi-contrast images is limited in accuracy due to potential mis-registration between images. Multi-echo SE sequences, such as turbo spin echo (TSE), are commonly used to speed up the acquisition. However, quantification is limited

because of contributions of stimulated and indirect echoes to the multi-echo signal, which depends on a variety of parameters including T_2, T_1, B_0, B_1^+ and diffusion. The accuracy of TSE-T_2 mapping can be improved by using a more complicated fitting approach, which accounts for all above-mentioned echo contribution effects, e.g. stepwise Bloch simulations, but this requires the pre-computation of a signal data base for fitting (10).

Alternatively, three-dimensional (3D) dual echo steady state (DESS) MRI (11–13) has shown its potential for T_2-mapping in the knee (14–16). DESS acquires two images ("FID" and "Echo") with distinct contrast in a single scan. This feature of DESS allows for both morphological T_2-weighted (T_2-w) and quantitative T_2 imaging in a single scan. Even though a simple exponential fit can yield quantitative T_2 if a flip angle (FA) of 90^o is used, to achieve sufficient SNR, DESS is typically performed at lower FA. As a consequence, T_2 mapping requires detailed modeling of the DESS signals (14–18).

We propose the application of DESS to achieve rapid 3D T_2 maps of the entire prostate. In this work, we aim to evaluate quantitative T_2 mapping with 3D DESS applied to the prostate in simulations, phantoms, healthy volunteers and a pilot patient study.

METHODS

This research was approved by the local institutional review board and all human subjects gave written, informed consent prior to scanning. MRI experiments were performed on a 3T MRI system (TIM Trio or Skyra, Siemens Healthcare, Erlangen, Germany) using a body matrix and a spine array coil. DESS was acquired in addition to standard T_2 mapping reference sequences (TSE in volunteers) and in addition to standard clinical sequences for prostate mp-MRI (in patients).

DESS Acquisition and T_2 Mapping

The DESS sequence is a steady-state free precession (SSFP) sequence, which acquires two signals in each TR: 1) "FID" with mixed T_2 /T_1 contrast and 2) "Echo" with primarily T_2 contrast (Figure 1). The ratio of these two signals was fitted to a signal model to obtain quantitative T_2 values for each image voxel (17). Detailed sequence

parameters are listed in Table 1. Quantitative T_2 mapping was performed in MATLAB R2013b (MathWorks, Natwick, MA, USA).

The signal ratio of DESS Echo and FID (*S*) shows a strong T_2 dependence (14–17,19), which is used to fit quantitative T_2. Since it also depends on T_1 and B_1^+, these parameters need either be measured to be included on a per voxel basis in the data fitting algorithm, or, in a simplified approach, a global (fixed) estimate for T_1 and B_1^+ can be used (16):

$$T_{2,fit} = \underset{\tilde{T}_2 \in T_{2,range}}{\operatorname{argmin}} \left\| S_{meas}(T_1, B_1^+, T_2) - S\left(T_{1,\mathrm{fix}}, B_{1,fix}^+, \tilde{T}_2\right) \right\|_2 \quad (1)$$

Where $S_{meas}(T_1,B^+_1,T_2)$ is the measured signal ratio and $S(T_{1,fix},B^+_{1,fix},T_2)$ are calculated from the signal model for each candidate T_2 in a predetermined range ($T_{2,range}$).

Simulations

In simulations, we sought to quantify the bias of fitted T_2 with respect to T_1 and B_1^+, if these were implemented as a fixed global estimate in a parameter range typically observed in prostate MRI. For the global estimate, we used $T_{1,\mathrm{fix}}$ = 2200 ms based on a recent study, which measured average T_1 in the prostate in 108 patients (20). We set relative $B_{1,\mathrm{fix}}^+$ = 1. Simulations were performed over a physiologically relevant parameter space. We assumed a range of $T_{1,\mathrm{true}}$ = [1500 to 3000 ms] and initially set $T_{2,\mathrm{true}}$ = 150 ms:

$$T_{2,fit}\left(T_{1,true}\right) = \underset{\tilde{T}_2 \in T_{2,range}}{\operatorname{argmin}} \left\| S_{sim}\left(T_{1,true}, B_{1,fix}^+, T_{2,true}\right) - S\left(T_{1,fix}, B_{1,fix}^+, \tilde{T}_2\right) \right\|_2 \quad (2)$$

Minimizing the cost function yields the result for fitted T_2 ("$T_{2,\mathrm{fit}}$"). The normalized difference between $T_{2,\mathrm{fit}}$ and $T_{2,\mathrm{true}}$ corresponds to the bias in the fitted T_2 estimate due to using a fixed T_1, which deviates from the true T_1:

$$T_2 bias_{T_{1,fix}}\left(T_{1,true}, T_{2,true}\right) = \frac{T_{2,fit}\left(T_{1,true}\right) - T_{2,true}}{T_{2,true}} \quad (3)$$

This simulation was expanded for a range of $T_{2,true}$ values ($T_{2,true}$ = [50 to 250 ms]) to obtain the T_2 bias over a range of $T_{1,true}$ and $T_{2,true}$. Similarly, simulations were also performed to study the T_2 bias due to relative B_1^+ variations over a range of 0.5 to 1.5.

Phantom Study

To verify our simulation results and to evaluate DESS-T_2 mapping performance in the presence of T_1 variations, we designed a phantom with 16 5-ml tubes filled with specific concentrations of Gd-DTPA and $CuSO_4$ to adjust the T_1 and T_2 relaxation times. The tubes were placed in a container filled with water and arranged in a 4x4 grid to comprise a range of T_1 values with variation along the column dimension and T_2 along the row dimension in a parameter range typically observed in the prostate: T_1 = 900 – 2000 ms, T_2 = 100 – 300 ms. We acquired 3D DESS and for reference T_2 mapping using 2D turbo spin echo with 9 TE values ranging from 12 to 270 ms. We also acquired a T_1 map using an inversion recovery turbo spin echo (IR TSE) sequence with 9 IR times ranging from 150 to 6000 ms to evaluate $T_{1,true}$ vs a global estimate $T_{1,fix}$ in the fitting algorithm. Other imaging parameters were identical to the volunteer study (Table 1). Quantitative T_2 maps were calculated from DESS as described above and from TSE data using a simple exponential fit. Similarly, quantitative T_1 was obtained from a simple exponential fit to the IR data. DESS T_2 fits were obtained in two ways: 1) using a global estimate for $T_{1,fix}$ = 2200 ms and 2) using a voxel based T_1 ($T_{1,true}$) derived from the IR T_1-map. For quantitative evaluation, ROIs were drawn in each tube. Median ROI values for DESS-T_2 were compared to TSE-T_2. Further, DESS-T_2 using $T_{1,fix}$ vs. a voxel-based T_1 map was compared. For repeatability analysis a second DESS-T2 acquisition was obtained 90 minutes later.

Volunteer Study

To evaluate prostate DESS T_2 mapping in vivo, four healthy male volunteers (27 ± 4 years) were scanned. To assess repeatability, three serial 3D DESS acquisitions (TA ~ 1 min each) were acquired. For reference, 2D turbo spin echo (TSE)-T_2 mapping was performed over a range of TE values (12 to 160 ms, total TA ~ 9 min). Detailed MR protocol parameters are listed in Table 1. Image analysis was performed in MATLAB.

For quantitative data analysis, ROIs were drawn in prostate peripheral zone (PZ), transition zone (TZ) and muscle (M) on three consecutive central image slices. ROIs were drawn on DESS-T_2 maps and copied to TSE-T_2 maps. If necessary, i.e. if the volunteer shifted between DESS-T_2 and TSE-T_2 acquisitions, ROIs were manually adjusted in 2 out of 4 volunteers by 1-2 pixels on TSE-T_2 to match DESS-T_2 ROI location using anatomical landmarks. Combining ROI data from all four volunteers and three image slices resulted in a total of n = 12 ROIs per zone. Median ROI values were compared between DESS-T_2 and TSE-T_2. Repeatability was assessed on serial DESS-T_2 scans.

Prostate Cancer Patient Study

As a clinical proof-of-principle study, 29 consecutive patients (58 ±18 years) were prospectively scanned with DESS after urologist referral for prostate mp-MRI. Men with elevated serum prostate-specific antigen (PSA) were referred for lesion detection prior to biopsy, or active surveillance (in men with biopsy proven low-grade cancer). Patient scans were conducted between June 2014 and March 2015. After obtaining informed consent, patients were scanned using the clinical standard mp-MRI protocol, and the DESS-T_2 mapping sequence was added (two serial 3D DESS scans, acquisition time for each scan was 1 min 3 s). In one patient, additionally, a high-resolution 3D DESS acquisition with image resolution matched to clinically acquired 3D T_2w TSE was added to show the clinical potential of DESS to replace T_2w-MRI. Table 1 lists the detailed MR protocol parameters of sequences relevant for this study. As part of clinical routine in our institute, a board-certified, experienced radiologist (>2000 cases read) identified suspected cancerous lesions on multi-parametric MRI based on criteria employed at our institute for prostate MRI readings (21): For T_2-w, ADC and DCE MRI, first an individual score for each of the three modalities ranging from 1-5 was assigned to a suspected MRI lesion (for scoring criteria see supporting Table S1). Finally, the overall suspicion level combining all three modalities was determined by the following formula: weighted average for final score = (2·ADC score + T2w score + DCE score)/4. If the combined score was 3 or greater, the lesion was termed “suspected cancerous lesion”.

For quantitative analysis, suspected cancerous lesion (SL) ROIs were drawn on clinical protocol 3D T_2-w TSE and re-drawn on DESS-T_2 maps matching the spatial ROI shape and location using anatomical landmarks. In addition to the SL ROI, ROIs were also drawn in normal peripheral zone (PZ), transition zone (TZ) and muscle (M). Similar to healthy volunteers, repeatability of the DESS-T_2 maps was also assessed by comparing serial DESS acquisitions. Further, to evaluate the dependence of DESS-T_2 on T_1 variations, DESS-T_2 obtained by using a fixed T_1 estimate ($T_{1,fix}$ = 2200 ms (20)) in the fitting algorithm was compared to DESS-T_2 using a pixel-based T_1 map (calculated from variable flip angle (VFA) T_1 mapping, MR protocol parameters see Table 1).

An additional feature of the DESS acquisition is that by combining the quantitative T_2-map and the DESS-FID acquired image with appropriate weighting factors, "synthetic" T_2-weighted images with any desired contrast weighting (TE_{eff}) can be calculated:

$$I_{TE_{eff}} = I_{DESS-FID} \cdot e^{-\left(\frac{TE_{eff}}{DESS-T_2}\right)} \quad (4)$$

Statistical Analysis

All statistical analysis was performed in MATLAB. All ROI results are presented as median ± standard deviation. Pooling ROI results for all volunteers or patients together, the mean ± standard deviation from all median ROI values was used. Linear regression and Pearson's correlation coefficient ρ was used to 1) compare DESS-T_2 to reference T_2 mapping (TSE), 2) assess repeatability on serial DESS-T_2 acquisitions and 3) evaluate the use of a global T_1 vs. pixel-based T_1 map. Differences between T_2 values in different ROI zones were tested with one-way analysis of variance and zone pairs were compared in a multiple comparison test with Bonferroni correction. A p-value of < 0.05 was considered significant.

RESULTS

Simulations

Our simulations showed that DESS-T_2 fitting using a global estimate for T_1 and B_1^+ is robust in the presence of T_1 and B_1^+ variations typically observed in prostate MRI. If the true T_1 or B_1^+ is smaller (larger) than the global T_1 or B_1^+ estimate, DESS-T_2 is under-(over) estimated (Figure 2a, c). The bias in T_2, due to T_1 or B_1^+ variations is more severe for larger T_2 (Figure 2b, d). However, results from a recent analysis of T_1 and B_1^+ in a representative patient population showed that over the whole prostate, T_1 variations were within 250 ms and B_1^+variations were within 10% (20). These observed parameter variations for T_1 (B_1^+) would translate to a bias in DESS-T_2 measurements of less than 2% (5%) (indicated by a red box in Figure 2).

Phantom Study

Quantitative IR TSE-T_1, TSE-T_2 and DESS-T_2 maps of the 4x4 T_1/T_2 phantom are shown in Figure 3 a-c. As intended by design, T_1 in the tubes was approximately constant along rows, but varied along the column dimension and vice versa for T_2. Assessing the T_1 dependence, phantom experiments confirmed our simulations results that using a fixed T_1 resulted in a bias in DESS-T_2 estimates (if T_1 true (from T_1 map) < T_1 fix (assumed) resulted in underestimation of DESS-T_2). This bias was increased for larger T_2 but within only a few percent over typical T_1 variations (Figure 3d). ROI analysis showed that DESS-T_2 was highly correlated to reference TSE-T_2 ($r^2 = 0.99$, p-value < 0.001) over a range of T_1 values (Figure 3e). Repeatability for DESS-T_2 in a scan-rescan experiment (after 90 min) was excellent ($r^2 = 0.99$, p-value < 0.001) (Figure 3f). The coefficient of variation was slightly higher for DESS-T_2 compared to TSE-T_2, however the difference was not significant (p-value = 0.23).

Volunteer Study

3D DESS images in a healthy volunteer exhibited distinctly different image contrast in the FID and Echo images (Figure 4a, b). From these images quantitative 3D DESS-T_2

maps were obtained (Figure 4c) and compared to reference 2D TSE-T_2 maps (Figure 4d). ROI analysis yielded DESS-T_2 of 115 ± 26 ms (mean ± SD of all volunteer ROI median values) in the PZ and 64 ± 7 ms in the TZ (Table 2, Figure 5a). A high correlation of DESS-T_2 and TSE-T_2 (r^2 = 0.88, p-value < 0.001, Figure 5b) was found. However, DESS-T_2 values were lower compared to TSE-T_2 values. This can be explained by the fact that our TSE-T_2 values were not corrected for contributions from stimulated echoes and achieving flip angles of less than 180° for the refocusing pulses in the multi-echo train. Both effects are known to result in T_2 overestimation on multi-echo based SE T_2 mapping (10). A high correlation of DESS-T_2 on serial scans (r^2 = 0.95, p-value < 0.001, Figure 5c) indicated high repeatability.

Prostate Cancer Patient Study

In 29 scanned patients, 23 suspected cancerous lesions were identified on standard mp-MRI in 17 patients. Only these men were included in further analysis. High-resolution DESS-Echo (Figure 6c) showed very similar T_2w contrast compared to clinical standard T_2w 2D TSE MRI (Figure 6b). DESS-FID and DESS-Echo images in patients showed clear depiction of morphological prostate zones, such as a distinction of PZ and TZ, on both contrast weightings (Figure 6c-f). These zones were also reflected in quantitative DESS-T_2 maps (Figure 6g). Quantitative ROI analysis yielded DESS-T_2 of 129 ± 39 ms (mean ± SD of all patient ROI median values) in the normal PZ and 83 ± 12 ms in the TZ (Table 2). DESS-T_2 in SL (72 ± 14 ms) was significantly different from normal PZ ($p < 0.001$, Figure 7a), but not from TZ T_2. DESS-T_2 on serial scans was highly correlated ($r^2 = 0.79$, p-value < 0.001, Figure 7b), even though the correlation was less than in healthy volunteers. We observed a very high correlation (r^2 = 0.99, p-value < 0.001, Figure 7c) of DESS-T_2 using a fixed T1 estimate ($T1_{fix}$ = 2200 ms) compared to DESS-T_2 using a pixel-based T1-map. From the quantitative DESS-T_2 map, we obtained flexible T_2-w contrast by calculating "synthetic" T_2-w images with TE_{eff} = 100 ms (Figure 6h).

DISCUSSION

Our results demonstrate that 3D quantitative T_2 mapping can be performed rapidly in the entire prostate using DESS at 3T with a spatial resolution of 1.1 x 1.1 x 3.5 mm^3 in about 1 min. We found a high correlation between DESS-T_2 and standard TSE-T_2 mapping approaches. There is a clear advantage using DESS with regard to total acquisition time, since a conventional T_2 mapping approach required about 9 min scan time.

Quantitative in vivo mapping of T_2 relaxation is still a challenge due to long scan durations. Multi-echo based T2 mapping (e.g., TSE) sequences are practical solutions to shorten the scan time, but they can be biased if stimulated echo contributions are not considered in the fitting algorithm and have considerably longer scan time than the DESS approach. Recently, acceleration techniques for multi-echo TSE have been proposed to reduce acquisition time three-fold from ~ 9 min to 2.8 min (22). Agarwal et al, combined k-t-T_2 with partial Fourier MRI and SENSE reconstruction to achieve 7.9 fold acceleration to obtain 0.60 mm in-plane 2D T_2 maps in a total acquisition time of 5 min 55 s to cover the whole prostate (23). For comparison, using 3D DESS to obtain the same image resolution would require 4 min 46 s without any acceleration techniques. Further, SAR is less of a concern for 3D DESS (FA=30°) compared to SE-type sequences, especially at 3 T.

Even though in this study we found in simulations and in vivo, that the bias in DESS-T_2 estimates due to "normal" T_1 variations over the prostate is small, this might not be the case for larger T_1 variations, for example present in hematoma, i.e. bleeding after biopsy. However, this residual bias can be eliminated by using voxel-based T_1 mapping, which is already part of clinical mp-MRI protocols because of its key role for quantitative DCE data analysis.

The prostate can be divided into different anatomical zones, which exhibit distinct tissue properties (24). The noncancerous, noninflamed peripheral zone is characterized by high macromolecular and free water content in luminal space, leading to longer T_2. Noncancerous central gland, including the transition zone has often a more heterogeneous appearance, especially when involved by benign prostatic hyperplasia, with overall

shorter T_2. This is reflected in our study results. We observed longer T_2 in the PZ as compared to the TZ for volunteers and patients using DESS-T_2. Further, our results using DESS-T_2 (129 ± 39 / 83 ± 12 ms in patient PZ and TZ) were in the same range as previously published T_2 values using TSE-T_2 mapping approaches at 3T (6,7,23,25,26). In addition, our result for muscle DESS-T_2 (38 ± 4 ms) compares well to muscle T_2 measured by Stanisz et al (40 ± 4 ms) at 3T (27). Cancerous tissue consists of highly compacted cells resulting in decrease in T_2. We found a significantly lower DESS-T_2 in suspected cancerous lesions (72 ± 14 ms) as compared to normal PZ tissue. Similarly, decreased T_2 in lesions was previously observed using spin echo mapping approaches (6,7,23,26). However, as it was recently pointed out by Langer et al. (28), although T_2 may help distinguish dense tumors from normal PZ tissue, bulk T_2 of sparse tumors (defined as intermixed prostate cancer with normal tissue) may not be significantly different from surrounding normal tissue. Therefore, the presence of normal PZ components in prostate cancer places inherent limitations on the ability of T_2 (and similarly to ADC within the mp-MRI protocol) to fully characterize PZ tumors.

The consensus for clinical prostate MRI interpretation recommends reviewing multi-parametric images in conjunction, including T_2-w, diffusion and dynamic contrast enhanced T_1-w images (29). The diagnostic performance of this multi-parametric approach may be potentially improved by the addition of a quantitative T_2 map. If done correctly, quantitative imaging yields a direct and repeatable assessment of tissue properties. The apparent diffusion coefficient (ADC) obtained from diffusion weighted imaging already adds a quantitative parameter to most clinical prostate MRI protocols and has been proven to be of great value in clinical prostate MRI (7,8,30–32). Quantitative T_2 may further enhance conventional multi-parametric quantitative analysis. Recent studies showed that quantitative T_2, similar to quantitative ADC, negatively correlated to cell density (12), however to a lesser extent as ADC. Therefore quantitative T_2 may facilitate noninvasive assessment of prostate cancer aggressiveness. For example, Wang et al found a correlation between signal intensity on T_2-w images with Gleason grade at whole mount pathologic evaluation after radical prostatectomy (33).

Even though the primary objective of this study was to present quantitative T_2 mapping, to be clinically relevant, the presented 3D DESS sequence must have potential to replace current T_2w imaging in the standard clinical protocol. This has already been demonstrated in an early study at 1.5 T (34). Also in our study, the "Echo" image showed similar contrast to current T_2w imaging. Further, using the DESS approach, any desired T_2 weighted image contrast can be retrospectively reconstructed using the quantitative DESS-T_2 map. A potential application of a "tunable" T_2 contrast image might be in post-processing algorithms such as automatic segmentation of the prostate as is required for studies comparing imaging results to whole-mount specimen analysis after prostatectomy.

Our study had several limitations. First, we only considered a single T_2 component in our analysis. However, recent studies have shown that prostate tissue in healthy volunteers can exhibit at least two T_2 components (35,36). DESS-T_2 mapping can be extended to a multi-component T_2 analysis if multiple DESS acquisitions, are acquired, thereby yielding more than two DESS-images for data fitting. Second, in our study we found significantly different T_2 in suspected cancerous lesion compared to PZ T_2. This might be important since most cancers are found in the PZ. On the other hand, we did not observe a significantly different mean T_2 in lesion compared to T_2 in the TZ. However, our patient population was small, potentially too small to lead to significant differences. Wang et al (33) found that lesions in the TZ classified as Gleason grade 3 had a significantly lower T_2 w signal intensity ratio than did lesions in the PZ classified as the same Gleason grade. As noted above, TZ prostate tissue appears more heterogeneous which potentially might hinder lesion detection based on quantitative imaging. Third, an important limitation of the DESS approach is the motion sensitivity of the acquisition sequence. This especially affects the "Echo" signal, which is lower in SNR. Our patients received Glucagon injection to reduce bowel movement. DESS T_2 -mapping could potentially greatly benefit from motion correction techniques. Finally, we did not correlate our quantitative T_2 results to histopathology or clinical outcome in this proof-of-principle patient study. This needs to be a topic of future research in large-scale patient studies, which could be accomplished using the fast 3D DESS T_2 mapping sequence as an add-on to standard prostate mp-MRI.

CONCLUSION

In conclusion, we have demonstrated that rapid one-minute 3D T_2 mapping of the entire prostate can be performed using DESS at 3T. Our results showed that DESS-T_2 was not sensitive to T_1, B_1^+ in a range typically observed in the prostate and has excellent repeatability. In an initial proof-of-principle patient study we have shown that DESS-T_2 in suspected cancerous lesions was significantly lower than in normal peripheral zone tissue. Based on our technique, the potential clinical impact of quantitative T_2 needs validation in further large-scale patient studies with multi-reader analysis and cross validation to histopathologic Gleason score and clinical outcomes.

ACKNOWLEDGEMENTS

The authors thank Sergio Godinez, Glen Nyborg, Pooria Khoshnoodi and Wei-Chan Lin for their assistance during the MRI exams.

REFERENCES

1. American Cancer Society. Cancer Facts & Figures 2015. Atlanta Am. Cancer Soc. 2015.

2. Ahmed HU, Kirkham A, Arya M, Illing R, Freeman A, Allen C, Emberton M. Is it time to consider a role for MRI before prostate biopsy? Nat Rev Clin Oncol 2009;6:197–206. doi: 10.1038/nrclinonc.2009.18.

3. Le JD, Tan N, Shkolyar E, Lu DY, Kwan L, Marks LS, Huang J, Margolis DJ a., Raman SS, Reiter RE. Multifocality and Prostate Cancer Detection by Multiparametric Magnetic Resonance Imaging: Correlation with Whole-mount Histopathology. Eur. Urol. 2015;67:569–576. doi: 10.1016/j.eururo.2014.08.079.

4. Salami SS, Ben-Levi E, Yaskiv O, Ryniker L, Turkbey B, Kavoussi LR, Villani R, Rastinehad AR. In patients with a previous negative prostate biopsy and a suspicious lesion on magnetic resonance imaging, is a 12-core biopsy still necessary in addition to a targeted biopsy? BJU Int. 2015;115:562–70. doi: 10.1111/bju.12938.

5. Liney GP, Knowles a J, Manton DJ, Turnbull LW, Blackband SJ, Horsman A. Comparison of conventional single echo and multi-echo sequences with a fast spin-echo sequence for quantitative T2 mapping: application to the prostate. J. Magn. Reson. Imaging 1996;6:603–607. doi: 10.1002/jmri.1880060408.

6. Liu W, Turkbey B, Sénégas J, Remmele S, Xu S, Kruecker J, Bernardo M, Wood BJ, Pinto P a, Choyke PL. Accelerated T2 mapping for characterization of prostate cancer. Magn. Reson. Med. 2011;65:1400–6. doi: 10.1002/mrm.22874.

7. Gibbs P, Liney GP, Pickles MD, Zelhof B, Rodrigues G, Turnbull LW. Correlation of ADC and T2 measurements with cell density in prostate cancer at 3.0 Tesla. Invest. Radiol. 2009;44:572–576. doi: 10.1097/RLI.0b013e3181b4c10e.

8. Langer DL, van der Kwast TH, Evans AJ, Trachtenberg J, Wilson BC, Haider M a. Prostate cancer detection with multi-parametric MRI: logistic regression analysis of quantitative T2, diffusion-weighted imaging, and dynamic contrast-enhanced MRI. J. Magn. Reson. Imaging 2009;30:327–34. doi: 10.1002/jmri.21824.

9. Chan I, Wells W, Mulkern R V, Haker S, Zhang J, Zou KH, Maier SE, Tempany CMC. Detection of prostate cancer by integration of line-scan diffusion, T2-mapping and T2-weighted magnetic resonance imaging; a multichannel statistical classifier. Med. Phys. 2003;30:2390–2398. doi: 10.1118/1.1593633.

10. Ben-Eliezer N, Sodickson DK, Block KT. Rapid and accurate T2 mapping from multi-spin-echo data using Bloch-simulation-based reconstruction. Magn. Reson. Med. 2014;00. doi: 10.1002/mrm.25156.

11. Bruder H, Fischer H, Graumann R, Deimling M. A New Steady-State Imaging Sequence for Simultaneous Acquisition of Two MR Images with Clearly Different Contrasts. Magn. Reson. Med. 1988;7:35–42.

12. Lee SY, Cho ZH. Fast SSFP gradient echo sequence for simultaneous acquisitions of FID and echo signals. Magn. Reson. Med. 1988;8:142–50.

13. Redpath TW, Jones R a. FADE--a new fast imaging sequence. Magn. Reson. Med. 1988;6:224–34.

14. Staroswiecki E, Granlund KL, Alley MT, Gold GE, Hargreaves BA. Simultaneous Estimation of T 2 and Apparent Diffusion Coefficient in Human Articular Cartilage In Vivo with a Modified Three-Dimensional Double Echo Steady State (DESS) Sequence at 3 T. Magn. Reson. Med. 2012;1096:1086–1096. doi: 10.1002/mrm.23090.

15. Welsch GH, Scheffler K, Mamisch TC, Hughes T, Millington S, Deimling M, Trattnig S. Rapid estimation of cartilage T2 based on double echo at steady state (DESS) with 3 Tesla. Magn. Reson. Med. 2009;62:544–9. doi: 10.1002/mrm.22036.

16. Heule R, Ganter C, Bieri O. Rapid estimation of cartilage T2 with reduced T1 sensitivity using double echo steady state imaging. Magn. Reson. Med. 2014;71:1137–1143. doi: 10.1002/mrm.24748.

17. Freed DE, Scheven UM, Zielinski LJ, Sen PN, Hürlimann MD. Steady-state free precession experiments and exact treatment of diffusion in a uniform gradient. J. Chem. Phys. 2001;115:4249. doi: 10.1063/1.1389859.

18. Wu E, Buxton R. Effect of Diffusion on the Steady-State Magnetization with Pulsed Field Gradients. J. Magn. Reson. 1990;253:243–253.

19. Bieri O, Ganter C, Scheffler K. Quantitative in vivo diffusion imaging of cartilage using double echo steady-state free precession. Magn. Reson. Med. 2012;68:720–9. doi: 10.1002/mrm.23275.

20. Zhong X, Rangwala N, Raman SS, Margolis DJ, Wu HH, Sung K. Clinical Assessment of B1+ Inhomogeneity Effects on Quantitative Prostate MRI at 3.0 T. In: International Society of Magnetic Resonance in Medicine Proceedings. ; 2015. p. accepted.

21. Sonn GA, Chang E, Natarajan S, Margolis DJ, Macairan M, Lieu P, Huang J, Dorey FJ, Reiter RE, Marks LS. Value of targeted prostate biopsy using magnetic resonance-ultrasound fusion in men with prior negative biopsy and elevated prostate-specific antigen. Eur. Urol. 2014;65:809–15. doi: 10.1016/j.eururo.2013.03.025.

22. Yamauchi FI, Penzkofer T, Fedorov A, Fennessy FM, Chu R, Maier SE, Tempany CMC, Mulkern R V., Panych LP. Prostate cancer discrimination in the peripheral zone with a reduced field-of-view T2-mapping MRI sequence. Magn. Reson. Imaging 2015. doi: 10.1016/j.mri.2015.02.006.

23. Agarwal HK, Sénégas J, Turkbey B, Bernardo M, Grant K, Boernert P, Merino M, Pinto P, Keupp J, Choyke PL. Whole-Prostate T2 Mapping in Under 6 Minutes for Prostate Cancer. 2012:4626.

24. McNeal JE. Regional morphology and pathology of the prostate. Am. J. Clin. Pathol. 1968;49:347–57.

25. De Bazelaire CMJ, Duhamel GD, Rofsky NM, Alsop DC. MR imaging relaxation times of abdominal and pelvic tissues measured in vivo at 3.0 T: preliminary results. Radiology 2004;230:652–659. doi: 10.1148/radiol.2303021331.

26. Langer DL, Evans AJ, Plotkin A, Trachtenberg J, Wilson BC, Haider MA. Prostate Tissue Composition and MR Measurements: Investigating the Relationships between ADC, T2, Ktrans, ve, and Corresponding Histologic Features. 2010;255:485–494.

27. Stanisz GJ, Odrobina EE, Pun J, Escaravage M, Graham SJ, Bronskill MJ, Henkelman RM. T1, T2 relaxation and magnetization transfer in tissue at 3T. Magn. Reson. Med. 2005;54:507–12. doi: 10.1002/mrm.20605.

28. Langer DL, van der Kwast TH, Evans AJ, Sun L, Yaffe MJ, Trachtenberg J, Haider MA. Intermixed normal tissue within prostate cancer: effect on MR imaging measurements of apparent diffusion coefficient and T2--sparse versus dense cancers. Radiology 2008;249:900–908. doi: 10.1148/radiol.2493080236.

29. Barentsz JO, Richenberg J, Clements R, Choyke P, Verma S, Villeirs G, Rouviere O, Logager V, Fütterer JJ. ESUR prostate MR guidelines 2012. Eur. Radiol. 2012;22:746–57. doi: 10.1007/s00330-011-2377-y.

30. Chamie K, Sonn G a., Finley DS, Tan N, Margolis DJ a, Raman SS, Natarajan S, Huang J, Reiter RE. The role of magnetic resonance imaging in delineating clinically significant prostate cancer. Urology 2014;83:369–375. doi: 10.1016/j.urology.2013.09.045.

31. Kozlowski P, Chang SD, Jones EC, Berean KW, Chen H, Goldenberg SL. Combined diffusion-weighted and dynamic contrast-enhanced MRI for prostate cancer diagnosis - Correlation with biopsy and histopathology. J. Magn. Reson. Imaging 2006;24:108–113. doi: 10.1002/jmri.20626.

32. Lawrence EM, Gnanapragasam VJ, Priest AN, Sala E. The emerging role of diffusion-weighted MRI in prostate cancer management. Nat. Rev. Urol. 2012;9:94–101. doi: 10.1038/nrurol.2011.222.

33. Wang L, Mazaheri Y, Zhang J, Ishill NM, Kuroiwa K, Hricak H. Assessment of biologic aggressiveness of prostate cancer: correlation of MR signal intensity with Gleason grade after radical prostatectomy. Radiology 2008;246:168–176. doi: 10.1148/radiol.2461070057.

34. Ikonen S, Kärkkäinen P, Kivisaari L, Salo JO, Taari K, Vehmas T, Tervahartiala P, Rannikko S. Endorectal magnetic resonance imaging of prostatic cancer: Comparison between fat-suppressed T2-weighted fast spin echo and three-dimensional dual-echo, steady-state sequences. Eur. Radiol. 2001;11:236–241. doi: 10.1007/s003300000598.

35. Storås TH, Gjesdal K-I, Gadmar ØB, Geitung JT, Kløw N-E. Prostate magnetic resonance imaging: multiexponential T2 decay in prostate tissue. J. Magn. Reson. Imaging 2008;28:1166–72. doi: 10.1002/jmri.21534.

36. Gilani N, Rosenkrantz AB, Malcolm P, Johnson G. Minimization of errors in biexponential T2 measurements of the prostate. J. Magn. Reson. Imaging 2015. doi: 10.1002/jmri.24870.

FIGURES

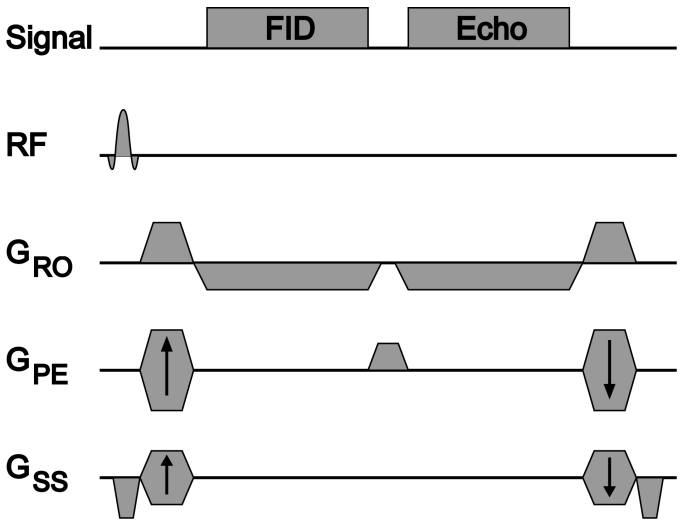

Figure 1. The DESS pulse sequence is a steady-state gradient echo sequence. In each TR two echoes with distinct image contrast are acquired, called the “FID" and the “Echo". A small spoiler gradient is applied between the FID and Echo signal to suppress banding artifacts.

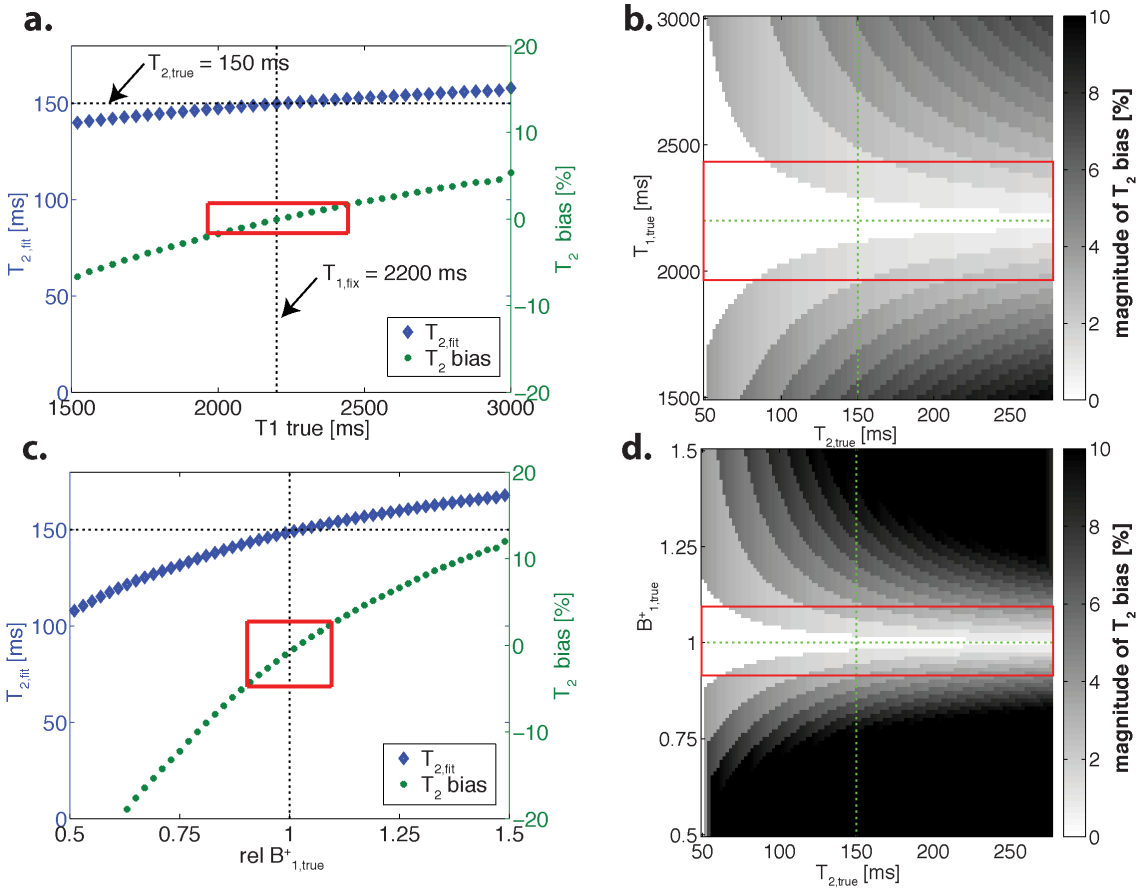

Figure 2: Simulations show that using a fixed T_1 estimate ($T_{1,fix}$ = 2200 ms) in the data fitting routine results in T_2 under- (over-) estimation ($T_{2,true}$ = 150 ms), if the true T_1 is lower (higher) than the T_1 estimate (a). If the true T_1 deviates from the T_1 estimate, the bias observed in the fitted T_2 -values is larger for increasing T_2 (b). Similar observations hold for B_1^+ variations (c,d). The simulated bias is within 2% (5%) for variations in T_1 (B_1^+) typically observed in the prostate (red box).

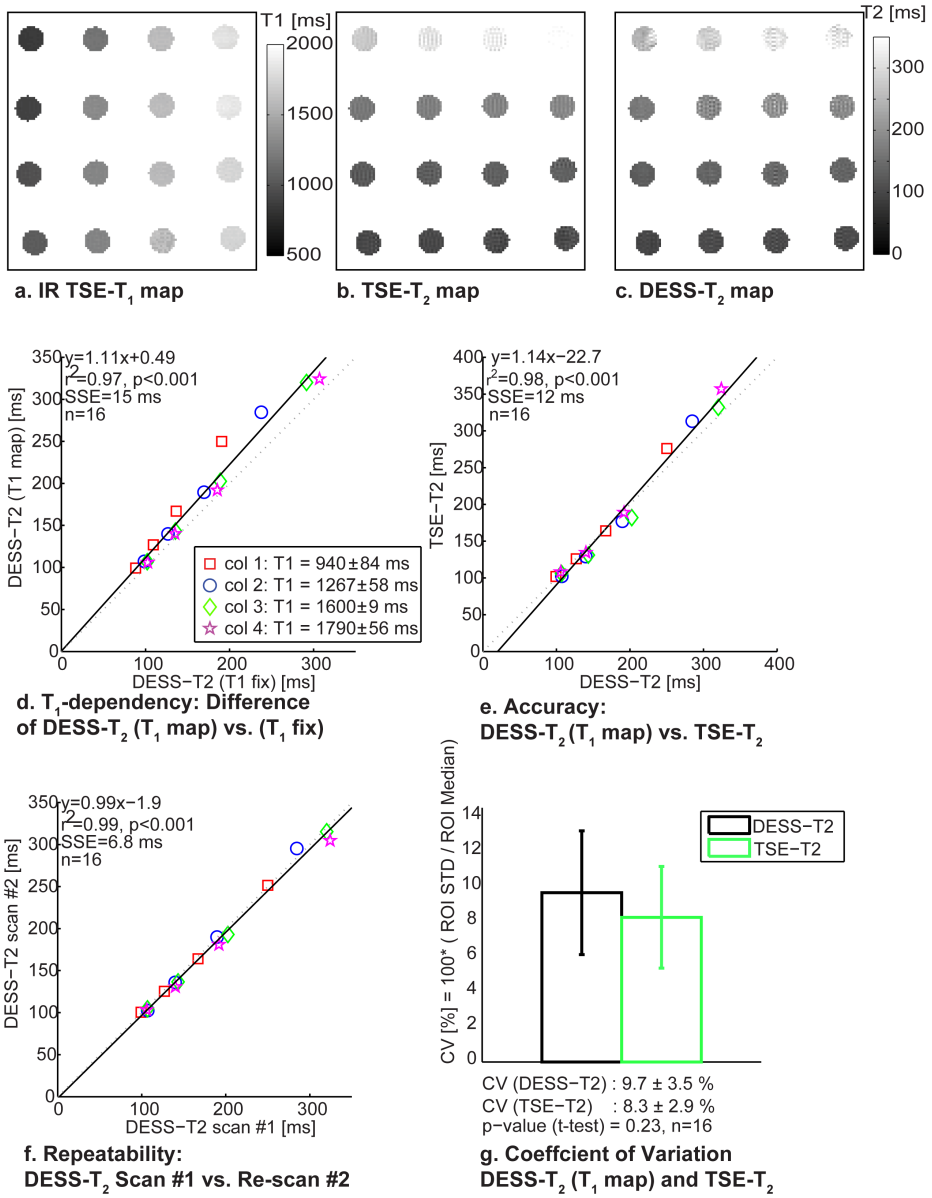

Figure 3: A phantom with T_1 / T_2 variations primarily along columns / rows was imaged using 2D Inversion Recovery (IR) turbo spin echo (TSE) T_1 mapping (a), 2D TSE-T_2 mapping (b) and 3D DESS-T_2 mapping (c). Using a fixed T_1 estimate (T_1 = 2200 ms) in the fitting routine, deviations in fitted T_2 values were found that were increased for larger T_2, consistent with simulation results (d). DESS-T_2 measurements were highly correlated with TSE-T_2 (r^2 = 0.98) over a range of T_1 values, using the T_1 map in the fitting routine (e). Scan-scan DESS-T_2 measurements showed excellent repeatability (f). The coefficient

of variation (CV) was higher for DESS-T_2 compared to TSE-T_2, however the difference was not significant (p-value = 0.23) (g).

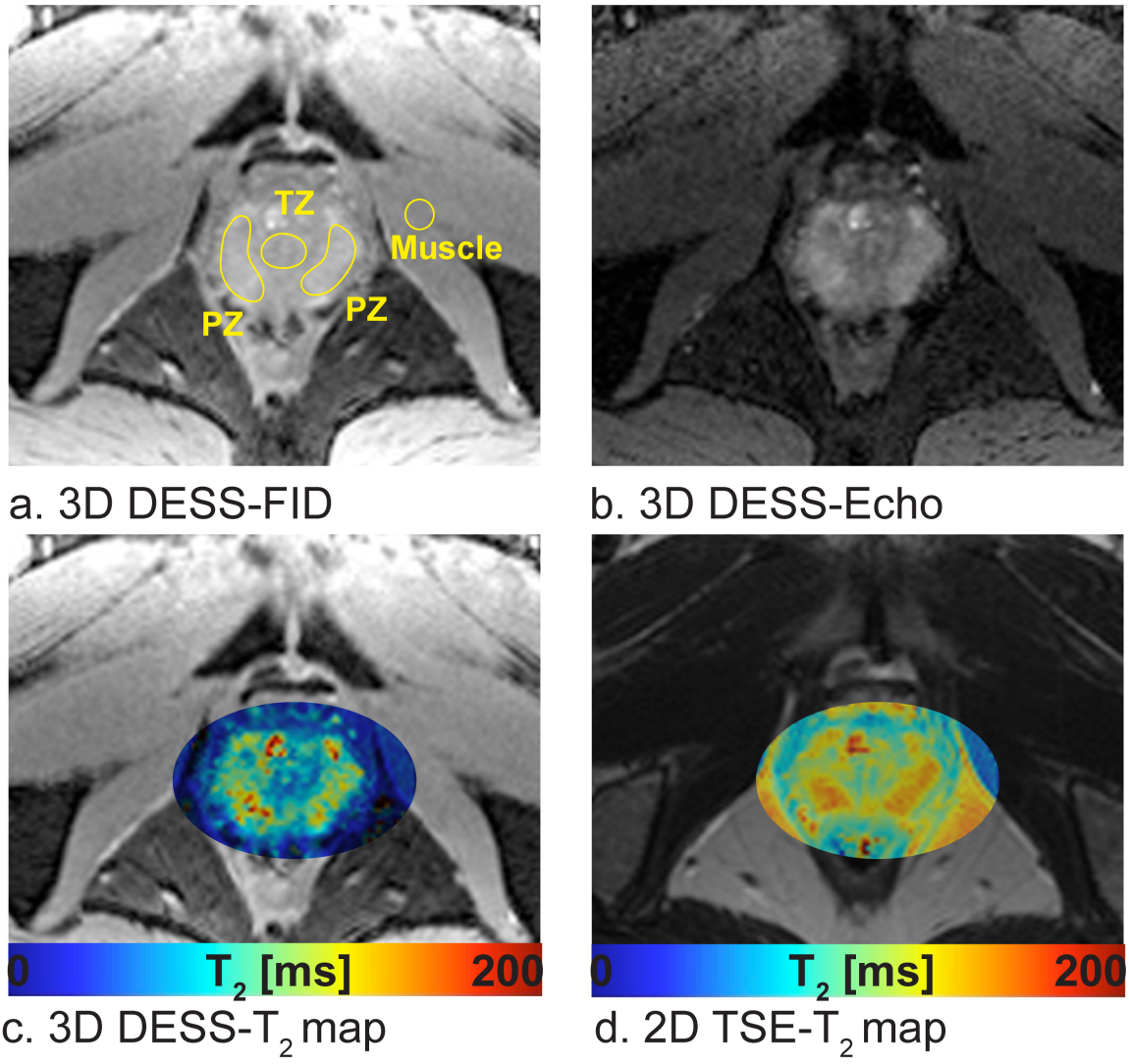

Figure 4: Representative DESS images from a healthy volunteer are shown: DESS-FID (a), DESS-Echo (b), DESS-T_2 map (c) and for comparison a TSE-T_2 map (d). DESS-FID and DESS-Echo are displayed at same window level settings. ROIs were drawn for further quantitative data analysis as shown in (a) in the peripheral zone (PZ), transition zone (TZ) and in muscle (M).

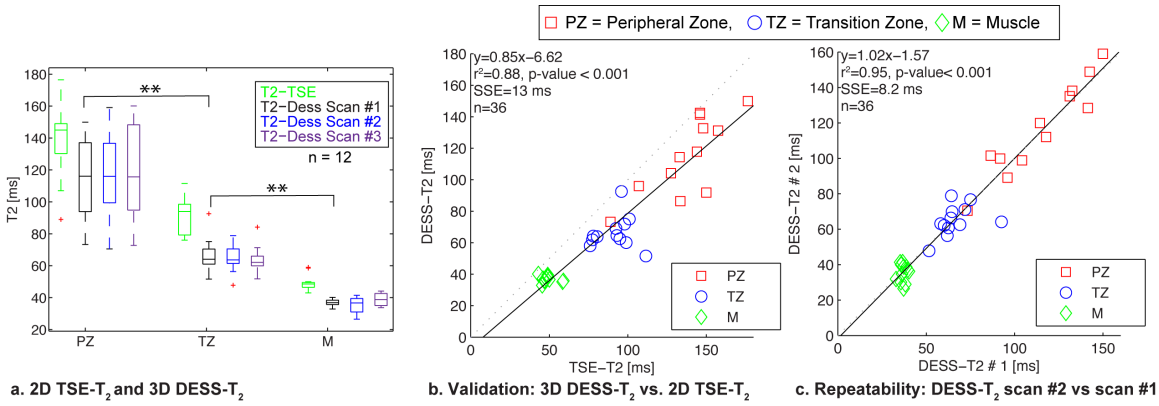

Figure 5: Results of quantitative analysis in healthy volunteers. Median T_2 values for the different ROI zones are shown for TSE-T_2 and 3 consecutive DESS-T_2 measurements (scan #1 to #3) (a). DESS-T_2 in all zones was significantly different from each other (p-value < 0.001), with larger DESS-T_2 in the PZ as compared to TZ. DESS-T_2 values (scan #1) were highly correlated with TSE-T_2 measurements (r^2 = 0.88, p-value < 0.001). Correlation of T_2 measurements obtained by two sequential DESS acquisitions was high (r^2 = 0.95, p-value < 0.001).

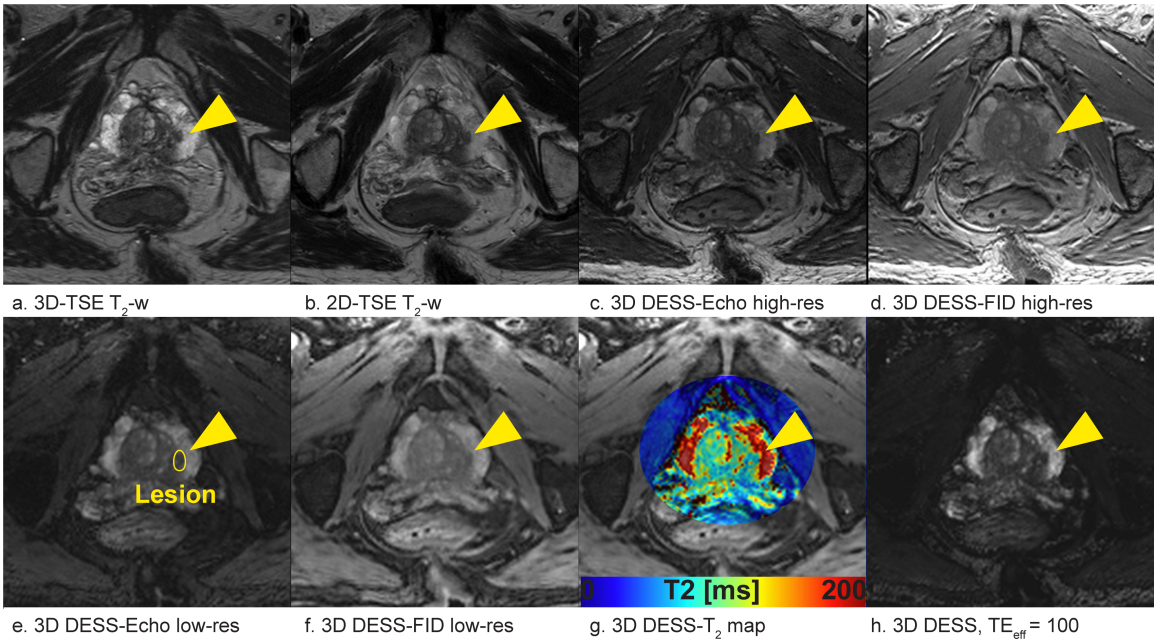

Figure 6: Representative DESS images from a prostate cancer patient compared to clinical standard T_2-w MRI: 3D T_2w TSE (a) and 2D-TSE T_2w (b) showed very similar T_2w contrast as high-resolution (0.66x0.66x1.5mm^3) 3D DESS-Echo (c). Simultaneously acquired high-resolution 3D DESS-FID (d) provided one additional contrast image. For T2-mapping, low-resolution (1.1x1.1x3.5 mm^3) 3D DESS-Echo (e) and DESS-FID (f) was fitted to obtain 3D DESS-T_2 map (g). DESS-FID and DESS-Echo are displayed at same window level settings. Retrospectively, using the DESS-T_2 map and the DESS-FID, 3D T_2-w images with desired "effective" TE contrast can be generated: e.g. TE_{eff} = 100 ms (h). A suspected cancerous lesion (indicated by a yellow arrow) identified by a radiologist on the clinical T_2-w images (a and b) is visually apparent in DESS images (c-h) and has low T_2-values (g). Note that a water excitation only pulse was used in low-resolution DESS (e,f) for fat suppression. For imaging parameters see Table 1.

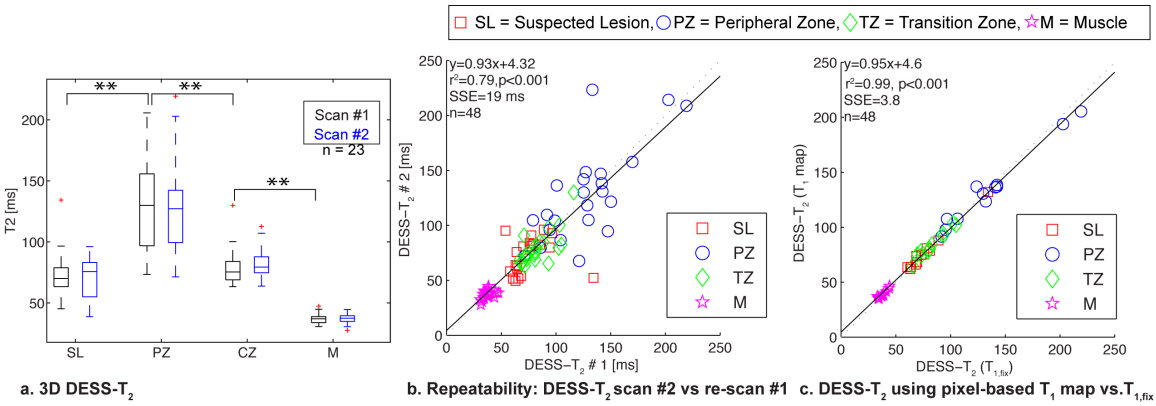

Figure 7: Results of quantitative analysis in prostate cancer patients. Median T_2 in SL ROIs was significantly different from PZ ROIs ($p < 0.001$) and but not from ROIs in the TZ (a). ROI T_2 values in repeated DESS scans were correlated ($r^2 = 0.79$, p-value < 0.001 (b)). There were no significant differences in T_2 if using a fixed T1 estimate (2200 ms) or a pixel-based T1 map ($r^2 = 0.99$, p-value < 0.001 (c)).

TABLES

Table 1: MR protocol parameters.

Study	Patient, Volunteer and Phantom: 3D DESS	Patient: high-resolution[b] 3D DESS	Patient: 2D T_2 w imaging	Patient: 3D T_2w imaging	Phantom and Volunteer: 2D T_2 mapping	Patient and Volunteer: T_1 mapping	Phantom: T_1 mapping
Sequence	DESS[a] (low-res)	DESS (high-res)	T_2w -TSE	3D T_2w-TSE	T_2 –TSE[c]	T_1-VIBE-Dixon[d]	T_1 –TSE[e]
Acquisition	3D	3D	2D	3D	2D	3D	2D
Fat Suppression	Water Excitation only						
Inversion Recovery Time							variable[e]
FOV [mm^2]	220x220	170x170	200x200	170x170	220x220	260x260	220x220
Image Matrix	192x192	256x256	310x320	256x256	192x192	160x160	192x192
Resolution [mmxmm]	1.1x1.1[f]	0.66 x 0.66[g]	0.6x0.6	0.66 x 0.66[g]	1.1x1.1	1.6x1.6	1.1x1.1
# PE Lines	287[h]	461[h]	651[h]	328[h]	192 (phantom), 308[h] (volunteer)	207[h]	192
Parallel Imaging (R)	2	2	-	2	-	-	-
Slice Thickness [mm]	3.5[f]	1.5[g]	3.6	1.5[g]	3.5	3.6	3.5
TR [ms]	18.56	19	4000	2200	4000	4.17	10500
TE [ms]	4.16	5	101	201	variable[c]	2.46	12
Flip Angle [°]	30	30	160	110	180	variable[d]	180
# Averages	1	2	2	2	1	3	1
Echo Train Length	-	-	25	-	22	2	22
Bandwidth [Hz/px]	160	160	200	315	130	895	130
Acquisition Time [min: sec]	1:03	7:26	3:20	7:00	0:31 (phantom), 1:02 (volunteer)	0:35	1:24

[a]DESS was acquired 3x (2x) in volunteers (patients) to assess repeatability.
[b]The resolution and FOV coverage of the high-resolution 3D DESS acquisitions were matched to clinically acquired 3D T2w TSE.

[c]T_2-TSE method for T_2 mapping: Sequence was repeated 9 times with TEs of [12, 25, 37, 61, 74, 09, 111, 135, 160] ms, total time ~ 9 min
[d]Variable Flip Angle (VFA) method for T_1 mapping: Sequence was repeated 4 times with a flip angle of 2°, 5°, 10° and 15°
[e]Inversion Recovery (IR)-TSE method for T_1 mapping: Sequence was repeated 9 times with inversion times of [50, 100, 150, 300, 500, 1000, 2000, 4000, 6000] ms
[f]For low resolution DESS, this is the acquired, raw image resolution, no interpolation.
[g]For high resolution DESS, matched to 3D T2-w imaging, this is the interpolated resolution (0.66 x 0.66 x 1.50 mm^3); the acquired resolution was (0.74 x 0.66 x 2.25 mm^3)
[h] Oversampling along phase-encode (right-left) dimension to avoid fold-over artifacts

Table 2: Quantitative DESS-T_2 values in healthy volunteers and patients (Median ± SD).

ROI zone[a]		SL	PZ	TZ	M
Volunteer[b]	TSE-T_2 [ms]		138 ± 23	92 ± 11	49 ± 5
	DESS-T_2 [ms]		115 ± 26	64 ± 7	37 ± 2
Patient[c]	DESS-T_2 [ms]	72 ± 14	129 ± 39	83 ± 12	38 ± 4

[a] For ROI location see Figure 4 and 6, SL = suspected cancerous lesion, PZ = peripheral zone, TZ = transition zone, M = muscle

[b] 12 ROIs were analyzed in healthy volunteers (n = 4, 3 image slices each)

[c] 23 ROIs were analyzed in prostate cancer patients (n = 17 patients, 1 slice per lesion)

SUPPORTING MATERIAL

Supporting Table S1:

Score	T_2-w TSE	ADC (x 10^{-3} mm^2/s)	DCE
1	Normal	> 1.4	Normal
2	Faintly decreased signal	1.2 – 1.4	Early or intense enhancement
3	Distinct low signal	1.0 – 1.2	Early and intense enhancement or early enhancement with washout
4	Distinct low signal with ill-defined margins	0.8 – 1.0	Early and intense enhancement with washout
5	Focal low signal with mass effect	< 0.8	Early enhancement is intense with immediate washout

Scoring criteria (1) for multi-parametric prostate MRI at our institution: T_2-weighted turbo spin echo (T_2-w TSE), apparent diffusion coefficient (ADC) mapping, dynamic contrast enhanced (DCE) MRI. First an individual score for each of the three modalities ranging from 1-5 was assigned to a suspected MRI lesion. The overall suspicion level combining all three modalities was determined by the following formula: weighted average for final score = (2·ADC score + T2w score + DCE score – TZ)/4 where "TZ" is 1 if the lesion lies in the transition zone and 0 otherwise. If the combined score was 3 or greater the lesion was termed "suspected cancerous lesion" and included in study.